Measurement of spatial resolution of 11 MeV proton radiography[*]

ZHANG Xiao-Ding (张小丁),[1,†] LI Yi-Ding (李一丁),[1] YANG Guo-Jun (杨国君),[1]
WEI Tao (魏涛),[1] HE Xiao-Zhong (何小中),[1] LONG Ji-Dong (龙继东),[1] JIANG Xiao-Guo (江孝国),[1]
MA Chao-Fan (马超凡),[1] ZHAO Liang-Chao (赵良超),[1] YANG Xing-Lin (杨兴林),[1]
ZHANG Zhuo (张卓),[1] WANG Yuan (王远),[1] LI Wei-Feng (李伟峰),[1] and SHI Jin-Shui (石金水)[1]

[1] *Institute of Fluid physics, China Academy of Engineering Physics, P.O. Box 919-106, Mianyang 621900, China*
(Received January 21, 2014; accepted in revised form May 24, 2014; published online December 15, 2014)

Proton radiography experiment with a Zumbro lens system was carried out on an 11 MeV proton cyclotron. The experimental results show that the image blurring is improved markedly. Clear images and good spatial resolution of the density step edges are obtained, which is important for hydrotest experiments, and the spatial resolution can achieve ∼100 μm.

Keywords: Proton radiography, Zumbro lens system, Spatial resolution

DOI: 10.13538/j.1001-8042/nst.25.060204

I. INTRODUCTION

Proton radiography (PRAD) is an advantageous method for hydrotests, with high penetrating power, high detection efficiency, small-scattered background, inherent multi-pulse capability, and large standoff distances between the object and detector [1–4]. The proton-materials interaction renders PRAD the capability of resolving higher density objects than flash x-ray radiography and identifying the materials. PRAD images can be used to evaluate interfaces, the position and velocity of the front of shock, and density transformation of test samples. The spatial resolution and areal density resolution of static objects are benchmark of working status of the imaging system.

In penetrating materials, the protons interact with electrons, the nuclear Coulomb field and the nucleus, hence the three effects: energy loss, multiple Coulomb scattering (MCS) and nuclear scattering. The MCS effect is the main cause of the blurring with low energy incident proton beams.

To eliminate this blemish, Zumbro and Thomas proposed a simple, elegant magnetic lens system to focus the scattered protons. Then, magnetic lens systems were designed for proton radiography experiments on the 800 MeV accelerator at Los Alamos Neutron Scattering Center (LANSCE) [5] and on the Alternating Gradient Synchrotron (AGS, 24 GeV proton beams) at Brookhaven National Laboratory [6]. The experimental results proved that this kind of lens system could reduce the image blurring remarkably. In their experiments, the spatial resolution was about 100 μm.

Protons in tens of MeV can penetrate samples in thicknesses of hundreds of microns, making the proton beams become a proper tool for imaging sub-mm samples. Also, PRAD may be used for imaging medical and biological samples. However, for low energy PRAD, the spatial resolution is a key parameter to get the sample information. In this paper, we report the proton radiography with unit magnification Zumbro magnetic lens system on an 11 MeV cyclotron. By analyzing the radiographed images of static objects, the spatial resolution of magnetic lens system is about 100 μm, which is an encouraging result for developing the technique for hydrotesting experiment.

II. METHODS

A. The chromatic cancellation of Zumbro lens system

The Zumbro lens system is a point-to-point image system with the unit magnification [7, 8]. Along the x and y direction, the transport transfer matrices are $-I's$. The system is composed of two identical doublets of quadrupole, which are reflection symmetric.

B. Blurring analysis

In radiography, the Zumbro lens system, the radiographed objects, the scintillator and the optical recording system all contribute to the image blurring. Blurring contributions from each part are considered as follows.

For the Zumbro lens system, the position-dependent chromatic aberrations, and the aberrations and blurring brought by the transport of proton beams, can be eliminated because that the lens works on the point-to-point radiography. However, for different spots of the sample, the chromatic aberration cannot be eliminated. The chromatic aberration blurring of different positions of the sample is calculated as [7]

$$B_{\text{lens}} = T_{126}\theta_0\delta, \tag{1}$$

where θ_0 is deviation angle of the MCS, $\delta = \Delta p/p_0$ is the momentum deviation, and T_{126} is element of transport matrix in TRANSPORT notation, which represents the second order chromatic aberration.

[*] Supported by National Natural Science Foundation of China (No. 11205144) and National Natural Science Foundation of China (No. 11176001)
[†] Corresponding author, zhangxiao_d@163.com

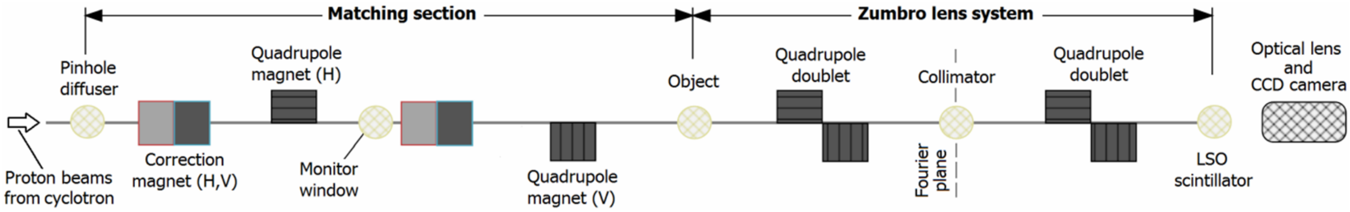

Fig. 1. (Color online) Schematics of the radiography beamline.

Before exiting the object, the protons have undergone millions of Coulomb scatterings, and angle distribution of the penetrating protons can be treated approximately as Gaussian distribution. The root-mean-square (rms) width, in milliradians, of MCS exit cone is

$$\theta_0 = [13.6/(p\beta c)](L/L_{\mathrm{R}})^{1/2}\{1 + [\log(L/L_{\mathrm{R}})]/9\}, \qquad (2)$$

where p is the beam momentum in GeV/c, βc is the velocity of the proton, L is the thickness of the object, and $L_{\mathrm{R}} \propto Z^2/A$ is the radiation length of the material [6]. So the blurring coming from the object can be considered as [9]

$$B_{\mathrm{obj}} = 3^{-1/2} L\theta_0. \qquad (3)$$

The blurring from the detection system, i.e. the scintillator and the downstream optical image system (the optical lens and the CCD camera) is denoted as B_{det}. Therefore, the total blurring can be calculated as,

$$B_{\mathrm{tot,FWHM}} = 2.36\left(B_{\mathrm{obj}}^2 + B_{\mathrm{lens}}^2 + B_{\mathrm{det}}^2\right)^{1/2}, \qquad (4)$$

where the coefficient 2.36 is obtained from the Gaussian distribution. This total blurring is the theoretical FWHM (Full Width at Half Maximum) of the edge differential image.

C. Experimental setup

The PRAD experiment for spatial resolution of the Zumbro lens system with static objects was carried out on the 11 MeV proton compact cyclotron [10], which provides average beam current of 50 μA. The collimated proton beam on the scintillator detectors was integrated from thousands of micro pulses in ten seconds or longer.

Figure 1 is a layout of the low energy PRAD imaging beamline [11]. It consists of a matching section, the magnetic lens system and the recording system. The matching section includes two correction magnets and two quadrupoles to make the beam matching to the magnetic lens system. The recording system includes a LSO scintillator at the image plane and a high resolution CCD camera about 15 cm downstream of the LSO scintillator.

The object was assembled by aluminium foils of different thicknesses and charcoal layer coated by a laser printer. Thickness of the charcoal layer was determined as follows: A 50 mm × 50 mm × 6 μm Al foil of known weight was coated with a charcoal of known density. It was weighed by an electric balance of 10 μg precision. Then, the averaged thickness of charcoal was determined as 4 μm.

A ϕ6 mm collimator was fixed on the Fourier plane, sorting the angle of scattered protons. Its maximum picking angle is 4.06 mrad in our experiment. The field of view (FOV) is larger than ϕ30 mm. The scintillator is a ϕ38 mm LSO (Lu_2SiO_4) screen, and the camera is a high quality industrial CCD camera.

III. EXPERIMENTAL DATA

Parameters of the imaging system are known or calculated. For example, $T_{126} = 2929mm$ is determined by the design of the Zumbro magnetic lens system, and the total blurring of the image beamline with an object of Al foil in thickness of 16 μm is estimated as follows: Because the object is too thin to affect the momentum deviation, the δ_{rms} should be momentum deviation of the cyclotron, which is about 0.003. A half of momentum deviation comes from the cyclotron and the other half comes from the diffuser. From Eq. (2), the MCS angle is $\theta_0 \sim 5.6$ mrad without the collimators. Therefore, the blurring from lens system is $B_{\mathrm{lens}} = 82$ μm. With the collimator, the rms of MCS angle changes. After the first doublet, the exiting protons are collected as a spot on the Fourier plane, the collimator on the spot position cuts off the protons with a smaller diameter, the maxima angle changes to the collimated angle. And on the scintillator, the angle θ is 3.38 mrad, and the blurring is $B_{\mathrm{lens}} = 29.73$ μm. For an Al foil of 9 μm thick, the blurring with the collimator can be estimated at $B_{\mathrm{lens}} = 29.70$ μm.

According to Eq. (3), the amount of 0.064 μm and 0.04 μm body blurring (B_{obj}) correspond to the 16 μm thick Al foil and the 9 μm thick Al foil, respectively.

From SRIM calculations, for 11 MeV protons travelling a 0.5 mm thick LSO scintillator, the lateral straggling is about 36 μm. The blurring B_{det} is about 36.9 μm. So in our experiment, from Eq. (4), the total blurring (FWHM) for Al foil of 16 and 9 μm in thickness is $B_{\mathrm{tot,FWHM}} \approx 112$ μm.

Figure 2 is the transmission image and edge position image of the stepped sample with a ϕ6 mm collimator on the Fourier plane. The density step positions in Fig. 2(b) are identified as those points where the gradient of image is the maximum. To get more precise position of the edge, we analyzed the red region in Fig. 2(a). By averaging the region along Y direction, and differentiating it along X direction, we had Fig. 2(c), and

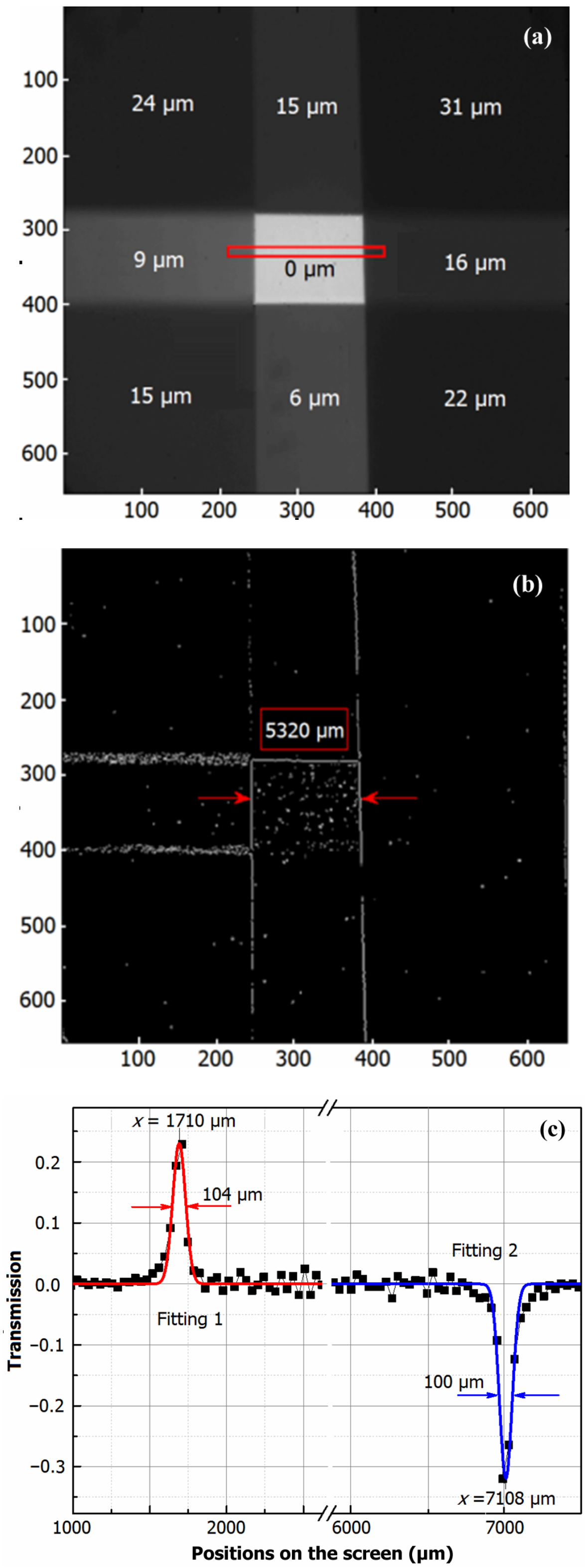

Fig. 2. (Color online) Proton transmission images of Al foils in thickness of 0, 6, 9, 15, 16, 22, 24 and 31 μm (a), the edge positions processed by MATLAB (b), and Gaussian fitting of differential vertical gray scale along the Fig. 2(a) red-line region (c).

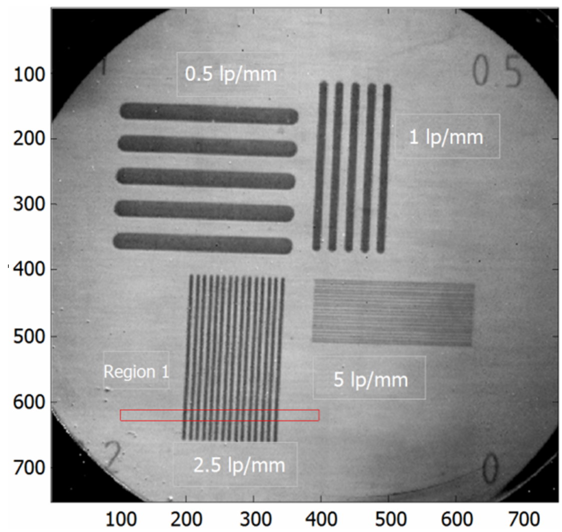

Fig. 3. (Color online) The transmission image of reticle radiography.

then made a Gaussian fitting with the differential peaks. The maxima of the differential peaks and the FWHM values were obtained. Comparing with the edge image, the peak is at the same position. FWHM of the peak is about 100 μm, which means that the spatial resolution of total imaging system is around 100 μm. The distance between two edges in Fig. 2(b) is 5 320 mm, while in Fig. 2(c), it is 5 308 mm. For the simple configuration, searching for the interface position of the differential using MatLab toolbox can provide cursory positions of the interface edges.

To obtain more direct information of the spatial resolution, check the spatial resolving power, and confirm the feasibility of searching for the interface position, reticle samples were radiographed. Fig. 3 shows transmission images of reticles of 0.5, 1.0, 2.5 and 5.0 lp/mm prepared with a laser printer on a 50 mm × 50 mm × 6 μm Al foil. We analyzed the intensity distribution and the derivative of the intensity distribution along the rectangle region.

In Fig. 3, the 2.5 lp/mm reticle can be distinguished clearly, and the 5 lp/mm reticles can also be distinguished by eyes, so 100 μm spatial resolution of the whole system can be achieved.

Comparing the results above, there is an inconsistency between the experimental data and the theoretical image blurring. They may come from the complex environment such as the vibration of vacuum pumps, and the jitter of proton beam. To obtain clearer radiography, efforts will be made for further understanding of the principle and working status of Zumbro lens system.

IV. CONCLUSION

We have performed the spatial resolution experiment of proton radiography on the 11 MeV cyclotron with a unit magnification Zumbro lens system. By analyzing the transmission image of reticle and edges image of Al foils, the data show that the imaging system can achieve the resolving power of 100 μm.

The results of this experiment are encouraging. They prove that the static radiography on the low current cyclotron is feasible. However, it is still a lot of work to improve spatial resolution of the system. For example, under bombardment of 11 MeV protons hit on, the scintillation occurs not in a point but a spot in the scintillator, so response characteristic of the scintillator needs to be studied. Similar efforts are needed for the collimator design, beam diagnosis of the cyclotron, and precise beam matching of the magnetic lens system. These shall be of great help for improving performance of the system.

[1] Burtsev V V, Lebedev A I, Mikhailov A L, *et al*. Combust Explo Shock+, 2011, **47**: 627–638.
[2] Shiberin I V, Batkov Y V, Burstev V V. XI Kharitonov Thematic Scientific Readings, Sarov, 2009, 304–309.
[3] Smilowitz L, Henson B F, Romero J J, *et al*. J Appl Phys, 2012, **111**: 103515.
[4] Morris C L, Hopson J W, Goldstone P. Los Alamos Science, 2006, **32**: 32–39.
[5] King N S P, Ables E, Adams K, *et al*. Nucl Instrum Meth A, 1999, **424**: 84–87.
[6] Morris C L, Ables E, Alrick K R, *et al*. J Appl Phys, 2011, **109**: 104905.
[7] Mottershead C T and Zumbro J D. Proceedings of the 1997 Particle Accelerator Conference, Vancouver, Canada, 1997, 1397–1399.
[8] He X, Yang G, Liu C. High Power Lase Part Beam, 2008, **20**: 297–300. (in Chinese)
[9] Wei T, Yang G J, Long J D. Chinese Phys C, 2013, **37**: 068201.
[10] He X, Yang G, Long J, *et al*. Nucl Tech, 2014, **37**: 010201. (in Chinese)
[11] Wei T, Yang G, Long J, *et al*. Chinese Phys C, 2012, **36**: 792–796.